Modeling of gas and aerosol with WRF/Chem over Europe: Evaluation and sensitivity study

Paolo Tuccella,[1] Gabriele Curci,[1] Guido Visconti,[1] Bertrand Bessagnet,[2] Laurent Menut,[3] and Rokjin J. Park[4]

[1] The "online" meteorological and chemical transport Weather Research and Forecasting/Chemistry (WRF/Chem) model has been implemented over a European domain, run without aerosol-cloud feedbacks for the year 2007, and validated against ground-based observations. To this end, we integrated the European Monitoring and Evaluation Programme (EMEP) anthropogenic emission inventory into the model pre-processor. The simulated average temperature shows a very small negative bias, the relative humidity and the wind speed are overpredicted by 1.5% (8%) and 1.0 m/s (76%), respectively. Hourly ozone (O_3) exhibits a correlation with observations of 0.62 and daily maxima are underestimated by about 4%. A general ozone underestimation (overestimation) is found in spring (fall), probably related to misrepresentation of intercontinental transport with time-invariant boundary conditions. Daily nitrogen dioxide (NO_2) is reproduced within $\pm15\%$ with a correlation of 0.57. Daily $PM_{2.5}$ aerosol mass shows mean bias of about -4.0 $\mu g/m^3$ (-7.3%), mainly attributable to the carbonaceous fraction. The model underpredicts particulate sulphate by a factor of 2, and overpredicts ammonium and nitrate by about factor of 2. Possible reasons for this bias are investigated with sensitivity tests and revealed that the aqueous phase oxidation of sulphur dioxide (SO_2) by hydrogen peroxide (H_2O_2) and O_3, missing in the configuration of WRF/Chem without aerosol-cloud feedbacks, explains the discrepancy.

Citation: Tuccella, P., G. Curci, G. Visconti, B. Bessagnet, L. Menut, and R. J. Park (2012), Modeling of gas and aerosol with WRF/Chem over Europe: Evaluation and sensitivity study, *J. Geophys. Res.*, *117*, D03303, doi:10.1029/2011JD016302.

1. Introduction

[2] In recent decades, aerosols have received much attention by scientists. Anthropogenic aerosol particles play a key role in climate system acting on the global radiation budget, directly by scattering and absorbing the incoming radiation or indirectly by altering the cloud properties [*Charlson et al.*, 1992; *Hansen et al.*, 1997; *Andreae et al.*, 2005; *Lohmann and Feichter*, 2005; *Rosenfeld et al.*, 2008]. Moreover, they contain carcinogens and toxins that cause cardiopulmonary disease [*Pope*, 2000] and premature mortality depending on exposure time [*Wilson and Spengler*, 1996].

[3] In continental Europe, the background annual average of particulate matter with aerodynamical diameter less than 10 μm (PM_{10}) and less than 2.5 μm ($PM_{2.5}$) mass concentrations are estimated as 7.0 ± 4.1 and 4.8 ± 2.4 $\mu g/m^3$

respectively, with the highest values observed in winter season [*Van Dingenen et al.*, 2004]. On average, PM_{10} exceeds the European 24-h limit value of 50 $\mu g/m^3$ more than 90 times a year at curbside sites, 18 at near-city and urban background sites [*Van Dingenen et al.*, 2004]. Chemical speciation analyses [*Putaud et al.*, 2004, 2010] show that organic matter (OM) is the major contributor to PM_{10} and $PM_{2.5}$ mass (15–30%) except at remote sites, where the sulphate contribution is larger (20–30%). Nitrate contributes 5–10% of PM_{10}–$PM_{2.5}$ mass at sites impacted by nearby pollution sources; in the Po Valley (Northern Italy) nitrate may reach 20% of PM mass. Elemental carbon (EC) contributes 5–10% of $PM_{2.5}$ throughout the boundary layer in Europe. Mineral dust may be a large fraction of PM_{10} at all types of site in Southern Europe, while sea salt may be a major component at natural coastal sites. Recent measurements carried out in the frame of CARBOSOL project (Present and retrospective state of organic versus inorganic aerosol over Europe: implication for climate) [*Legrand and Puxbaum*, 2007] show that 50–60% of organic carbon (OC) is water –soluble, which might be mostly attributed to secondary sources [*Pio et al.*, 2007]. *Gelencsér et al.* [2007] have conducted an analysis to provide a source apportionment of organic aerosol. In summer, a large part of OC is found to originate from biogenic sources, with 63–76% of total carbon (TC) composed of secondary organic aerosols

[1]CETEMPS, Department of Physics, University of L'Aquila, L'Aquila, Italy.
[2]Institut National de l'Environnement Industriel et des Risques, Verneuil en Halatte, France.
[3]Laboratoire de Météorologie Dynamique, Institut Pierre-Simon Laplace, Ecole Polytechnique, Palaiseau, France.
[4]School of Earth and Environmental Sciences, Seoul National University, Seoul, South Korea.

Table 1. WRF/Chem Configuration[a]

Process	WRF/Chem OPTION
Microphysics	Lin
Long-wave radiation	RRTM
Short-wave radiation	Goddard
Surface layer	Monin-Obukhov
Land-surface model	Noah LSM
Boundary layer scheme	MYNN Level 2.5 PBL
Cumulus parameterization	Grell-Devenyi
Photolysis scheme	Fast-J
Gas-phase mechanism	RADM2
Aerosol model	MADE/SORGAM

[a]Please refer to the model user's guide for a complete description of the options.

(SOA) from oxidation of non-fossil hydrocarbons. On the other hand, the origin of elemental carbon (EC) is dominated by fossil sources throughout the year. In particular, in winter the main source appears to be from wood burning [*Gelencsér et al.*, 2007].

[4] In recent years, many Chemistry-Transport Models (CTM) have been developed to better understand the physical-chemical processes of gas-phase species and particulate matter and are also being applied for operational air quality forecasts. A few examples of CTM applied at the European scale are EMEP [*Simpson et al.*, 2003], TM5 [*Krol et al.*, 2005], CHIMERE [*Bessagnet et al.*, 2008], LOTOS-EUROS [*Schaap et al.*, 2008], REMOTE [*Langmann et al.*, 2008], REM-CALGRID [*Stern et al.*, 2006], EURAD [*Memmesheimer et al.*, 2004], BOLCHEM [*Mircea et al.*, 2008], and POLYPHEMUS [*Sartelet et al.*, 2007]. Results from several models have been recently intercompared over Central Europe [*Stern et al.*, 2008] and over four large cities [*Vautard et al.*, 2007]. The authors found that the models generally satisfactory reproduce ozone, but underestimate $PM_{2.5}$ and PM_{10} mass concentrations by 4.0–14.0 $\mu g/m^3$ (10–50%) and 6.5–18.0 $\mu g/m^3$ (20–50%) respectively.

[5] CTMs are typically implemented in "offline" configuration, i.e. meteorological input is provided by an independent model, and thus not able to simulate the complex aerosol-cloud-radiation feedbacks. Moreover, the decoupling between the meteorological and chemical model leads to a loss of information, because of the physical and chemical processes occurring on a time scale smaller than the output time step of the meteorological model (typically 1 hour) [*Zhang*, 2008]. *Grell et al.* [2004] showed that most of the model variability in vertical velocity is attributable to higher frequency motions (period less than 10 minutes), yielding to much larger errors in vertical mass distribution in offline models with respect to "online" models, where meteorological and chemical processes are solved together on the same grid and with the same physical parameterizations [*Zhang*, 2008].

[6] In this paper, we report on a first validation of a European implementation of the new coupled meteorology-radiation-chemistry WRF/Chem model [*Grell et al.*, 2005]. We use the model without the full coupling of aerosol and cloud processes, because the complex feedbacks may complicate the interpretation of results on gas and aerosol phase simulations. This work is thus aimed at a preliminary validation of the model for future application to the study of the aerosol-clouds interactions. In section 2, we describe the

model and the interface to the EMEP anthropogenic emissions we implemented. In section 3, we evaluate the model performance looking at the comparison of a one year simulation (year 2007) with measurements of meteorology and chemical composition. A subsection is dedicated to sensitivity tests to explore the model bias in the simulation of the particulate secondary inorganic fraction. Concluding remarks are given in final section 4.

2. Model and Observations Description

2.1. WRF/Chem Model

[7] In this study, the version 3.2 of the air quality model WRF/Chem is implemented over Europe. The Weather Research and Forecasting (WRF) Model is a mesoscale non-hydrostatic meteorological model that includes several options for physical parameterizations of Planetary Boundary Layer (PBL), land surface, and cloud processes (www.wrf-model.org). WRF/Chem is a version of WRF coupled "online" with a chemistry model where meteorological and chemical components of the model are predicted simultaneously. A complete description of the model is given by *Grell et al.* [2005] and *Fast et al.* [2006].

[8] The main options for physical and chemical schemes adopted here are listed in Table 1. These include the Noah Land Surface Model [*Chen and Dudhia*, 2001], the Mellor-Yamada Nakanishi-Niino boundary layer scheme [*Nakanishi and Niino*, 2006], the Grell-Devenyi cumulus parameterization [*Grell and Devenyi*, 2002], the Lin microphysics scheme [*Lin et al.*, 1983], the Goddard shortwave radiation scheme [*Chou et al.*, 1998] and the Rapid Radiative Transfer Model (RTTM) longwave radiation scheme [*Mlawer et al.*, 1997]. The gas phase chemistry model used is the Regional Acid Deposition Model, version 2 (RADM2) [*Stockwell et al.*, 1990], that includes 57 chemical species and 158 gas phase reactions, of which 21 are photolytic. The aerosol module includes the Modal Aerosol Dynamics Model for Europe (MADE) [*Ackermann et al.*, 1998] for the inorganic fraction, and the Secondary Organic Aerosol Model (SORGAM) [*Schell et al.*, 2001] for the carbonaceous secondary fraction. MADE/SORGAM in WRF/Chem uses the modal approach with three log-normally distributed modes (nuclei, accumulation and coarse mode).

[9] The aerosol species treated in MADE/SORGAM are the main inorganic ions (NH_4^+, NO_3^-, SO_4^-), elemental carbon (EC), organic matter (OM, primary and SOA), aerosol water, sea salt and mineral dust. The photolysis frequencies are calculated with the Fast-J scheme [*Wild et al.*, 2000], the dry deposition velocities are simulated with the parameterization developed by *Wesely* [1989]. A simplified parameterization for wet scavenging in convective updrafts is included for main trace gases and inorganic aerosols. The full wet deposition module, coupled with aqueous chemistry, available in WRF/Chem is not included in our study, because these two processes cannot be activated separately from aerosol indirect effects. Consequently, the conclusions of this paper could be affected by a simplified parameterization of an important sink such as the wet scavenging.

[10] We simulate the whole year 2007 over Europe on a coarse grid that extends from 35° N to 57° N in latitude and from 15° W to 27° E in longitude. The horizontal resolution is 30 km and 28 vertical levels extend up to 50 hPa (about

20 km). The initial and boundary meteorological conditions are provided by the European Centre for Medium-range Weather Forecast (ECMWF) analyses with an horizontal resolution of 0.5° every 6 hours. The chemical boundary conditions of trace gases consist of idealized, northern hemispheric, mid-latitude, clean environmental profiles based upon the results from the NOAA Aeronomy Lab Regional Oxidant Model (NALROM) [*Liu et al.*, 1996]. The vertical profiles of the main trace gases are reported in auxiliary material Table S1.[1] The NALROM model simulates the chemistry with the lumped species which are separated into the individual model species of RADM2 using appropriate apportionment fractions. For example, O_x corresponds only to O_3 of RADM2 and the NO_x is split into 75% as NO and 25% as NO_2 . NH_4^+ and NO_3^- are set to a constant mixing ratio, the $SO_4^=$ is obtained from the H_2SO_4 profile, assuming that a fraction of the latter is converted to the aerosol sulfate. The simulation is carried out at 72 hours time-slots, starting at 1200 UTC of a given day and then run for 84 hours, with first 12 hours discarded as model spin-up. The chemical state of the model is restarted from previous run, while meteorology is reinitialized from global analysis. The first 16 days of simulation (15–31 December 2006) are used as spin-up for chemistry.

[11] WRF/Chem has demonstrated its ability to reproduce ozone in different situations with RADM2 and MADE/SORGAM: over North America [*Grell et al.*, 2005], during rapidly changing weather conditions in Shanghai (China) [*Tie et al.*, 2009], in Mexico City [*Zhang and Dubey*, 2009] and in Southern Italy (for gas-phase only) [*Schürmann et al.*, 2009], where air circulation is strongly affected by the complex orography. Previous studies also show that the model is able to simulate the aerosols over North America. *McKeen et al.* [2007] evaluating the real time forecasts of $PM_{2.5}$ with several models, reported that WRF/Chem bias depends on several factors such as the emission inventory used, the horizontal resolution and parameterizations of the PBL turbulence. Including direct and indirect aerosol effects with CBM-Z gas-phase mechanism [*Zaveri and Peters*, 1999] and MOSAIC aerosol model [*Zaveri et al.*, 2008], *Zhang et al.* [2010] show that over the continental US WRF/Chem exhibits a $PM_{2.5}$ bias from −7% to +30% in January, and 8–30% in July.

2.2. Emissions

[12] Anthropogenic emissions are taken from the European Monitoring and Evaluation Program (EMEP) data base (www.ceip.at/emission-data-webdab/emissions-used-in-emep-models), which provide total 2007 annual emission of nitrogen oxides (NO_x), carbon monoxide (CO), sulphur oxides (SO_x), ammonia (NH_3), Non-Methane Volatile Organic Compounds (NMVOC), and particulate matter ($PM_{2.5}$ and coarse PM) over Europe with a resolution of 50 km for 11 sources types (SNAP sectors) [*Vestreng*, 2003]. The procedure followed to build the emissions interface is derived from that of the CHIMERE model [*Bessagnet et al.*, 2008]. Emissions are distributed on height levels depending on the SNAP sector [*Vestreng*, 2003]. Time variability is calculated with monthly and hourly emission profiles provided by the IER (University of Stuttgart)

[*Friedrich*, 1997]. *de Meij et al.* [2006] show that, over Europe, the high temporal resolution of emissions does not influence strongly the concentrations of aerosol mass, with the exception of aerosol nitrate and its gas-phase precursor NO_x and NH_3. However, *Wang et al.* [2010] demonstrate that when the vertical and temporal distributions of emissions are considered, WRF/Chem better reproduces the surface observations of key trace gases.

[13] Total amount of NMVOC emissions is disaggregated into several species using UK speciation profiles [*Passant*, 2002]. Aggregation of NMVOC species into RADM2 model species is done in two steps, following the procedure proposed by *Middleton et al.* [1990]. The NMVOC obtained from Passant speciation are first lumped on a mole-to-mole basis into 32 chemical groups, according to their expected impact on oxidants and acid formation, and then aggregated into RADM2 model species, applying the reactivity weighting factor principle.

[14] SO_x emissions are split into 95% as SO_2 [*Chin et al.*, 2000; *Simpson et al.*, 2003] and 5% as particulate sulphate ($SO_4^=$): the latter is distributed for 20% into nuclei mode and for 80% into the accumulation mode. $PM_{2.5}$ emissions are assigned to unspeciated primary $PM_{2.5}$ model species, and also distribute for 20% into nuclei mode and for 80% into accumulation mode. Coarse PM emissions are assigned to PM_{10} model species.

[15] Elemental carbon (EC) and organic carbon (OC) emissions are taken from 2000 total annual data emissions provided by the Laboratoire d'Aerologie (www.aero.obs-mip.fr) and are treated the same way as EMEP data. EC and OC emissions are assumed to be for 20% in nuclei mode and for 80% in accumulation mode of corresponding model species. The conversion factor used to convert the emissions of OC to OM is 1.6 [*Bessagnet et al.*, 2008].

[16] Auxiliary material Figure S1 shows the maps of the average NO_x and the sum of all anthropogenic NMVOC emissions in July over the European domain of WRF/Chem. It is possible to see the strong gradients between rural and industrialized/urban areas and the emissions from major shipping tracks over the seas.

[17] Biogenic VOC emissions are calculated on line with a module based on the Guenther scheme [*Guenther et al.*, 1993, 1994]. Dust [*Shaw et al.*, 2008] and sea salt emissions are also included in the simulation.

2.3. Measurements

[18] Simulation results are compared to meteorological and chemical observations. Meteorological observations are part of the Integrated Surface Database (ISD) of National Oceanic and Atmospheric Administration (NOAA, http://www.ncdc.noaa.gov/oa/climate/isd/index.php), which consists of global synoptic surface observations provided as hourly averages. The meteorological observations include also the radiosonde profiles provided by the National Center for Atmospheric Research (NCAR) Earth Observing laboratory atmospheric sounding data (http://weather.uwyo.edu/upperair/sounding.html).

[19] Surface chemical measurements are provided by EMEP database (http://tarantula.nilu.no/projects/ccc/emepdata.html). EMEP stations are representative of regions characterized by background concentrations. The distribution of the network is shown in auxiliary material Figure S2.

---

[1]Auxiliary materials are available in the HTML. doi:10.1029/2011JD016302.

Table 2. Comparison of WRF/Chem Simulation Over Europe in 2007 Against Ground-Based Meteorological and Chemical Observations[a]

Variable	Stations	Mean Obs	Mean Mod	r	MB	MNBE (%)	MNGE (%)
			Meteorology				
Temperature (°C)	321	12.3	12.2	0.89	−0.1	−1.6	20.7
Relative Humidity (%)	314	73.6	75.3	0.65	+1.5	+8.0	19.6
Wind Speed (m/s)	293	3.4	4.4	0.55	+1.0	+76.1	96.5
Wind Direction (Deg)	231	195.6	194.7	0.38	45.9	47.6	47.6
			Gas Phase				
O_3 ($\mu g/m^3$)	75	65.0	63.7	0.62	−1.4	+36.8	57.6
Max 1-h O_3 ($\mu g/m^3$)	75	84.6	76.0	0.71	−8.6	−4.4	19.8
Max 8-h O_3 ($\mu g/m^3$)	75	78.9	73.1	0.70	−5.8	−0.2	21.4
NO_2 ($\mu g/m^3$)	27	7.0	6.1	0.57	−0.9	+14.9	63.2
NH_3 ($\mu g/m^3$)	11	1.3	0.9	0.46	−0.5	−3.5	78.4
HNO_3 ($\mu g/m^3$)	7	1.2	2.3	0.30	+1.1	+177.6	210.1
SO_2 ($\mu g/m^3$)	29	1.2	1.6	0.47	+0.4	+165.5	185.8
			Aerosol				
$PM_{2.5}$ ($\mu g/m^3$)	19	12.6	8.6	0.41	−4.0	−7.3	59.6
NH_4^+ ($\mu g/m^3$)	21	1.8	1.7	0.57	+0.5	+96.4	139.0
NO_3^- ($\mu g/m^3$)	25	2.9	4.4	0.48	+1.5	+115.2	169.3
SO_4^- ($\mu g/m^3$)	51	2.4	0.9	0.50	−1.5	−46.9	64.9
EC ($\mu g/m^3$)	4	1.3	0.4	0.44	−0.9	−51.2	65.4
OM ($\mu g/m^3$)	4	3.3	0.8	0.28	−2.5	−73.6	77.5

[a]Values are averaged over all available stations, Please refer to Appendix A for the definition of the statistical indices. In auxiliary material Figures S6–S22 we further show the box-whiskers plots of the indices.

Measurements are given as daily means, with the exception of ozone which is reported as hourly averages.

[20] We include in our analysis only the stations having 75% of annual data coverage, with the exception of $PM_{2.5}$ and aerosol inorganic mass concentration measurements for which a less restrictive threshold of 40% is applied. For HNO_3, NH_3, EC and OC measurements we use all available stations. We take into account the aerosol organic mass (OM) multiplying the observed OC by a factor of 1.6 [*Turpin and Lim*, 2001; *Bessagnet et al.*, 2008]. We point out that the statistical evaluation of some variables is performed with a limited number of stations, preventing us to have robust statistics. The number of station available for each examined variable is reported in Table 2.

3. Results

[21] In this section, we compare model simulations with observed ground-based data. The aim is to assess the skill of WRF/Chem in simulating meteorological variables, the main trace gases, and particulate matter mass and chemical composition. The statistical indices used here are the correlation coefficient (r), the mean bias (MB), the mean normalized bias error (MNBE) and the mean normalized gross error (MNGE). For the complete definition of the indices please refer to Appendix A.

3.1. Meteorology

[22] The simulated temperature, relative humidity, wind speed and wind direction are compared with NOAA surface measurements. In Figure 1 we show the comparisons of predicted time series (left panels) with hourly measurements, averaged over all available stations. The average diurnal cycle (right panels) with the 25th and 75th percentiles (red bar and shadow area) is also shown. The analysis of percentiles distribution is useful to understand if the model is

able to capture the dynamic range of the observations [*Mathur et al.*, 2008; *Kasibhatla and Chameides*, 2000]. In Table 2 we show the statistical indices of comparison averaged over all stations. Since the statistical indices averaged over all stations may mask their variability, in auxiliary material Figures S6–S22 we also show the box-whisker plots of the statistical indices.

[23] The temperature is simulated with a correlation of 0.89 and a small negative bias of −0.1°C, due to underestimation of daily maxima. Looking at the annual time series, a cold bias is typical for the spring-summer period and a warm bias for the winter-fall.

[24] The model reproduces the relative humidity with a correlation of 0.65 and a small bias of +8%, due to minimum values around noon, consistently with the underestimation of temperature maxima. An overestimation of minima is also noticed in spring-summer.

[25] The model systematically overestimates wind speeds by about 1 m/s (+76%), but the diurnal cycle is well reproduced. This high relative wind bias was previously reported for WRF/Chem [*Zhang et al.*, 2010], and is attributable to enhanced relative differences at the lower end of the wind speed distribution (auxiliary material Figure S3). The wind direction bias is calculated as the angle between observed and simulated directions, and it displays a mean value of 46°.

[26] The simulated meteorological quantities are also compared with atmospheric radiosonde observations. In Figure 2 we compare the domain average of predicted and observed vertical profiles recorded at 00 and 12 UTC, with shaded areas denoting the 25th and 75th percentiles, of simulated and observed distributions. While the temperature is overestimated up to 700 hPa, the relative humidity is underpredicted along the profile. *Misenis and Zhang* [2010], studying the sensitivity of WRF/Chem to various PBL and land-surface parameterization, found that the vertical profiles of temperature and relative humidity are very sensitive to
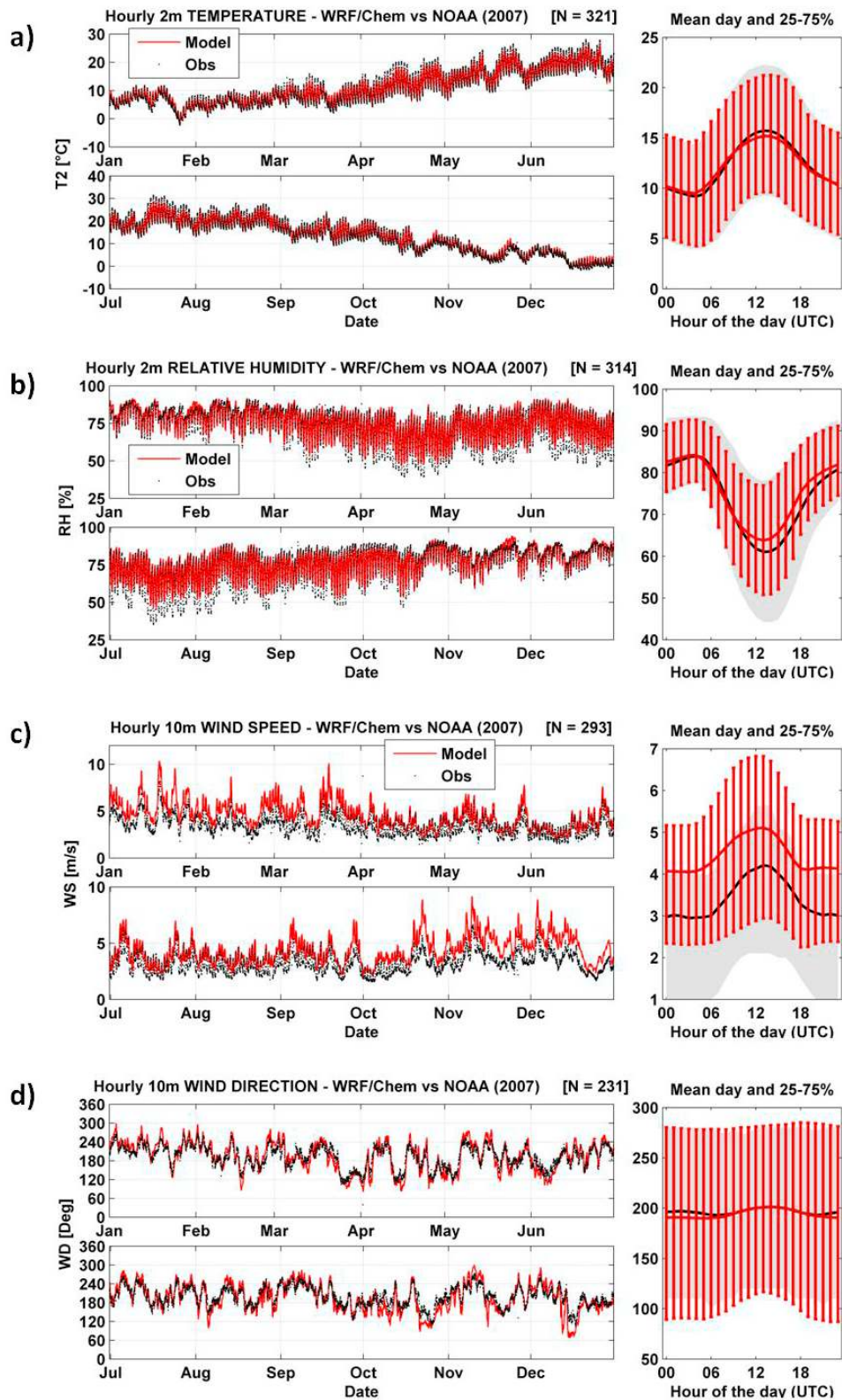
Figure 1. Comparison of meteorological variables time-series observed (black) at ground-based stations (NOAA Integrated Surface Hourly database) and simulated with WRF/Chem (red) for year 2007. (left) Time-series average at all available stations, and (right) the average daily cycle with the mean (solid line) and 25th and 75th percentiles (shaded area and bars). (a) Temperature at 2 m, (b) relative humidity at 2 m, (c) wind speed at 10 m, and (d) wind direction at 10 m.
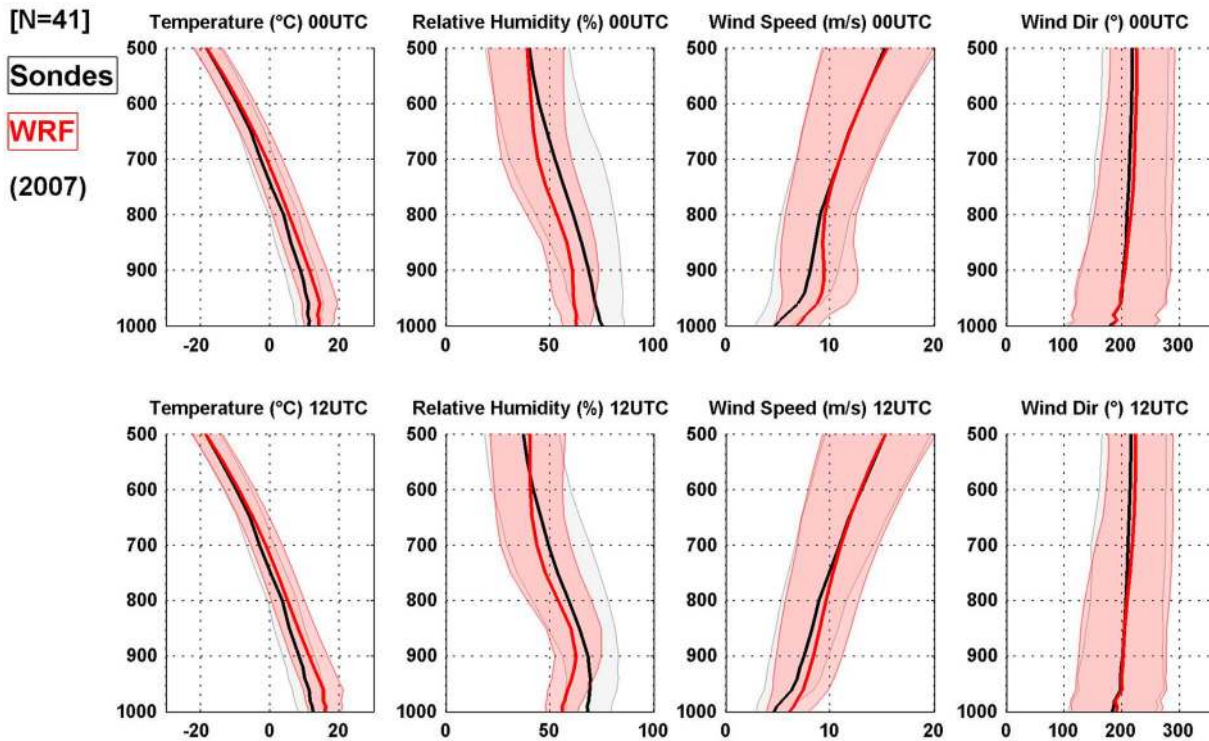
Figure 2. Comparison of meteorological variables vertical profiles observed (black) at station of National Center for Atmospheric Research (NCAR) Earth Observing laboratory atmospheric sounding data and simulated with WRF/Chem (black) for year 2007. Values are averaged over all stations. The shadow areas are the 25th and 75th of the distribution.

the adopted schemes. The model captures the profile of the wind speed in the upper levels and tends to overestimates it in the bottom layers, confirming the overestimation noticed in the comparison with ground-based observations. This bias is greater at 00 than at 12 UTC. The wind direction is well simulated over the whole atmospheric profile.

[27] The errors in temperature and relative humidity simulation may affect chemical transformation rates and aerosol formation processes. The discrepancies among modeled and

observed wind field may lead to errors in the location of pollutant accumulation areas.

3.2. Gas-Phase Chemistry

[28] Figure 3 shows the domain average of the comparison among observed and modeled O_3 at EMEP stations. A negative bias is found in daytime and the variability, as indicated by the percentiles, is not fully captured by the model. The tendency of the model to overestimate (underestimate) the
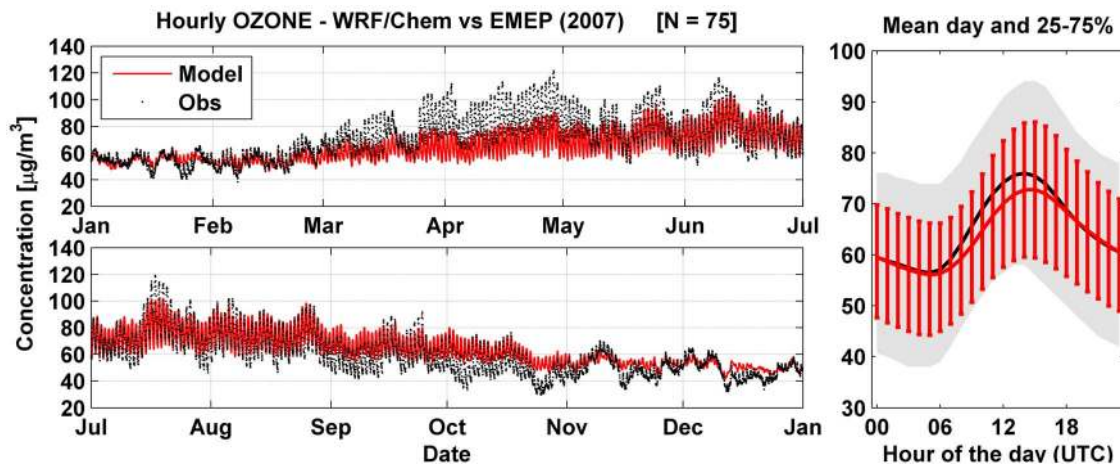
Figure 3. Same as Figure 1 but for comparison of observed and simulated hourly ozone at EMEP ground stations.
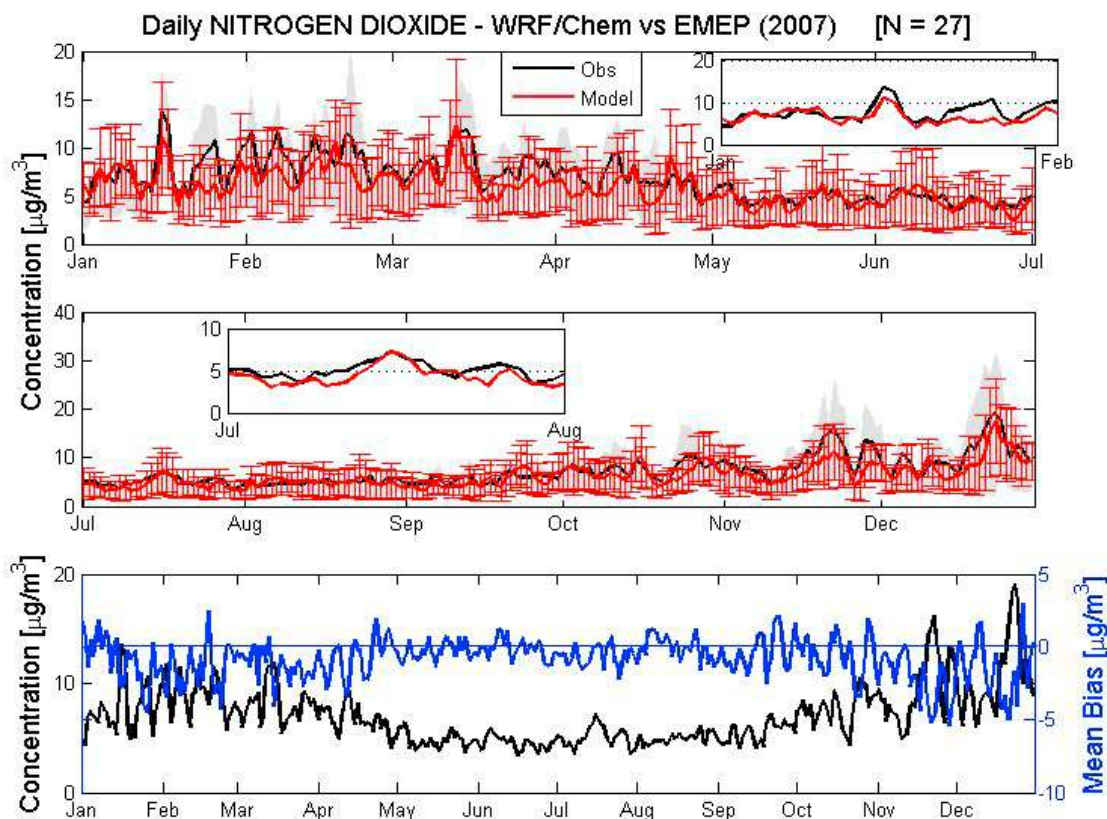
Figure 4. Comparison of nitrogen dioxide daily observations (black) at EMEP stations with WRF/Chem simulations (red). Values are averaged over all available stations. (top and middle) Mean (solid line) and 25th and 75th percentiles of time series are shown (red bars and shaded area). (bottom) The mean observed time series (black) and the mean model bias (blue).

lower (higher) end of the observed distribution is confirmed by the scatter plot in auxiliary material Figure S4. The best agreement is found in summer months, while in winter lowest values are overestimated. A noticeable underestimation (overestimation) is found in spring (fall). One possible reason of the discrepancy may be sought into a misrepresentation of background ozone levels. This calls into cause the static model boundary conditions used in WRF/Chem standard version used here (see section 2.1), that might be inadequate to describe the monthly variability of O_3 low-level inflow from North America, especially in spring [*Auvray and Bey*, 2005]. Several studies showed that the agreement with measurements of simulated O_3 improves when time-dependent boundary conditions are included in place of static profiles (see *Curci* [2012] for a review). We performed a sensitivity simulation in the period 15 March–15 May with doubled values of O_3 boundary conditions on the western border of the domain. Auxiliary material Figure S5 shows the results. In several periods of the simulation, it is evident how the model is sensitive to the influx from western border, which may compensate the model low bias alone. The issue warrants further study in the future.

[29] The model simulates the hourly O_3 with a correlation ranging from 0.38 to 0.83 (auxiliary material Figure S10) and a mean value of 0.62, a bias of -1.4 $\mu g/m^3$ and a relative bias of +36%. The different sign of MB and MNBE is due to the higher relative difference at lower end of distribution with respect to the higher end (auxiliary material Figure S4). The ozone maxima calculated over 1-hour and 8-hours are underestimated by 8.6 $\mu g/m^3$ and 5.8 $\mu g/m^3$, respectively, while the correlations are 0.70 and MNGE about 20%. A closer inspection to the auxiliary material Figures S11 and S12 reveals that the positive and negative values of MNBE cancel out. Consequently, the values of MNGE are always larger with respect to the absolute values of MNBE. This is a common feature for some of the chemical variables listed in Table 2. However, the model underestimation of ozone maxima calculated over 1-hour and 8-hours is evident in the box-whisker plots of the concentrations. The statistical indices obtained for the ozone are comparable with those reported in the ozone models inter-comparison by *van Loon et al.* [2007]. They found correlations ranging from 0.64 to 0.80 for ozone daily means and from 0.72 to 0.84 for the daily maxima. Over eastern North America, *McKeen et al.* [2005] show that in summer WRF/Chem simulates the 1 h and 8 h maxima ozone with a median correlation of 0.64 and 0.67 respectively, and with a positive bias of about 6–7 $\mu g/m^3$.

[30] Figure 4 compares the domain average of simulated and observed NO_2 daily mean, with red bars and shaded area denoting the 25th and 75th percentiles of simulated and observed distributions, respectively. In lower panel, the time series of model mean bias is also shown. WRF/Chem is able to reproduce the seasonal and day-to-day variations of NO_2
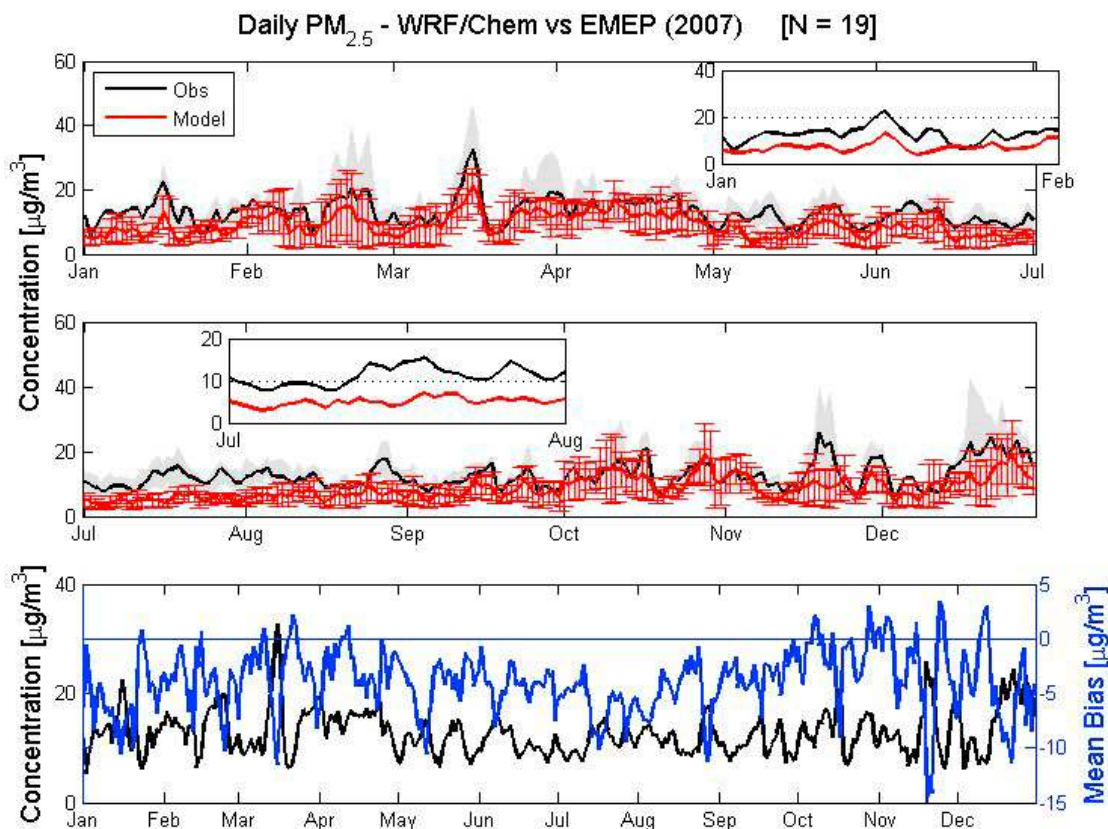
Figure 5. Same as Figure 4 but for daily $PM_{2.5}$.

concentrations, but the highest values are underpredicted. NO_2 simulation show a bias of -0.9 $\mu g/m^3$ (+15%) and the correlation with measurements is in the range of 0.2 to 0.81 (auxiliary material Figure S13) with a mean value of 0.57. The different sign of MB and MNBE is due to the same reason discussed for ozone; moreover, as noted for O_3, the positive biases balance the negative biases and the values of MNGE are larger than those of MNBE (auxiliary material Figure S13). The mean bias shows a seasonal dependence with a model tendency to underestimate (overestimate) during the cold (warm) season. Larger model errors are found in correspondence of days with the highest NO_2 observed concentrations. Over Europe, *Stern et al.* [2008] reported correlations with NO_2 observations in the range of 0.1 to 0.42 in the frame of their model inter-comparison.

3.3. Particulate Matter

[31] Figure 5 presents the comparison among observed and modeled domain average daily $PM_{2.5}$ concentrations, with 25th and 75th percentiles. The time series of model bias is also shown. We found a systematic negative model bias throughout the year, especially in July and August. The model captures the variability induced by some pollution episodes (e.g. mid March or end of November), but underestimates their magnitude. The analysis of percentile values displayed in Figure 6, better show that the underestimation is mostly attributable to the higher end of concentrations distribution. The correlation with observations ranges from -0.2 to 0.69 (auxiliary material Figure S17) with a mean

value of 0.41 and the mean bias is about -4.0 $\mu g/m^3$ (-7.3%).

[32] These results are consistent with other aerosol modeling studies. In their inter-comparison over Europe, *Stern et al.* [2008] report model correlations between 0.37 and 0.57, and bias in the range of -13.50 $\mu g/m^3$ to $+7.64$ $\mu g/m^3$. During summer 2004, over Eastern United States, *Yu et al.* [2008] evaluating the performances of Eta-CMAQ modeling system in forecasting the $PM_{2.5}$, found a correlation range from 0.58 to 0.70 and a MNBE of about -20%.

[33] In order to explore the reasons of negative bias in modeled $PM_{2.5}$, we analyze the simulation of the $PM_{2.5}$ chemical speciation. Figure 7 shows the simulated and observed time series of daily $PM_{2.5}$ mass concentration, secondary inorganic ions (NH_4^+, NO_3^-, $SO_4^=$) and their gas phase precursors (NH_3, HNO_3, SO_2) at Langenbrügge station (DE0002R, Germany). Ammonia does not present a systematic bias, while ammonium is biased high in cool months and close to observations in summer. The model underpredicts HNO_3 in winter time and overestimates it in summer, while simulated NO_3^- shows a very high positive bias in all seasons. Modeled SO_2 generally presents a positive bias, while $SO_4^=$ is biased low during all year.

[34] Generally, we found model biases similar to Langenbrügge station at other EMEP stations. Statistical summary of the comparison is given in Table 2, while in Figure 8 we compare observed and modeled annual mean aerosol composition. WRF/Chem simulates the NH_4^+, NO_3^- and $SO_4^=$ with a correlation of 0.57, 0.48 and 0.50 respectively.
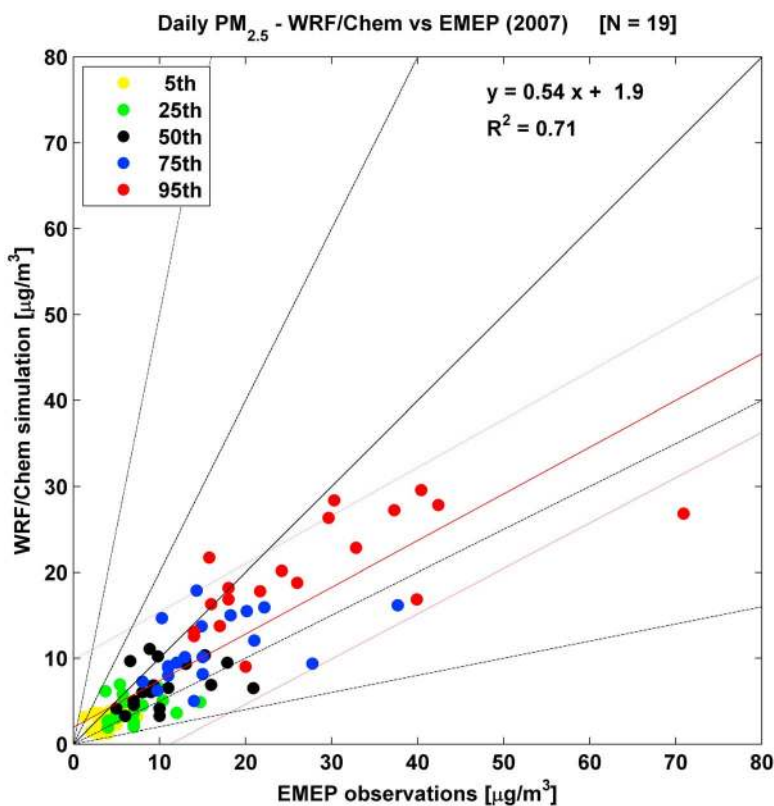
Figure 6. Comparison of observed and simulated daily $PM_{2.5}$ concentrations for year 2007. At each monitoring station, the percentiles of the distribution of observed and simulated time series are calculated and paired on the scatter plot. The lines 1:1, 2:1 and 4:1 are shown for reference. Best least-squares linear fit with corresponding uncertainty (red lines), regression line values and coefficient of determination (R^2) are also shown.

Simulated NH_4^+ and NO_3^- have a mean bias of 0.5 $\mu g/m^3$ (+107%) and 1.5 $\mu g/m^3$ (+115%), respectively, while $SO_4^=$ is underestimated by −1.5 $\mu g/m^3$ (−50%). Auxiliary material Figures S18–S20 show the variability range of the statistical indices relative to the inorganic aerosols. The overestimation of NO_3^- is a consequence of the underestimation of $SO_4^=$, because not enough ammonia is consumed by sulfate, thus favoring the formation of ammonium nitrate (NH_4NO_3) [Meng et al., 1997; Seinfeld and Pandis, 2006]. The reasons of $SO_4^=$ model underestimation are further investigated in section 3.4.

[35] The most noticeable error in $PM_{2.5}$ simulation is attributable to the carbonaceous aerosol fraction. Even if the definition of EC/OC in models and measurement is not always unique and consistent [e.g., Vignati et al., 2010] the low bias of the model is evident. The modeled EC mass is about a factor 3 lower than observed. A potential model bias may derive from the observation that EC at EMEP rural sites is mostly attributable to transport from urban sites [Putaud et al., 2004], that cannot be accurately resolved at a coarse resolution of 30 km. Modeled OM has a MB of −2.5 $\mu g/m^3$ a MNBE of +74%. Furthermore, it must be considered that the measurement uncertainties may be up to a factor 2 for EC and up to ±30% for OC [Schmid et al., 2001]. Finally, we point out that the analysis of carbonaceous aerosols is based on a very small number of stations (four) that prevent us from having a robust statistics. Moreover, this limited

data set also includes the Montelibretti station (IT0001R, Italy) that is not representative of rural areas [Carbone et al., 2010]. To compensate the scarcity of measurements, we perform a qualitative comparison among the model results and the data of EC and OM available in literature. The data used are the measurements of EC and OC issued from the EMEP 2002–2003 campaign [Yttri et al., 2007] and OM data reported by Jimenez et al. [2009].

[36] The underestimation of simulated EC is confirmed in the Po Valley (where the observed values of EC are the greatest in Europe [Yttri et al., 2007]), where the modeled and measured annual mean concentrations are of 0.4–1.0 $\mu g/m^3$ and 1.5–1.8 $\mu g/m^3$, respectively. The model underprediction of OM is also confirmed. The simulated annual mean concentrations of OM range from 0.5 to 3.5 $\mu g/m^3$, while the concentrations observed at EMEP sites are between 1.7–10.9 $\mu g/m^3$ and the values reported by Jimenez et al. [2009] are in the range of 1.9–9.3 $\mu g/m^3$.

[37] For the purpose of our analysis, it is also interesting to explore qualitatively how well the model reproduces the SOA and their relative amount compared to total OM. WRF/Chem predicts SOA annual mean concentrations of about 0.02–0.18 $\mu g/m^3$, while the observations indicate values of 0.5–8.0 $\mu g/m^3$ [Jimenez et al., 2009]. The simulated SOA/OM ratio has values of 5–40% against 50–80% observed. One of the most probable reasons for OM underestimation is that the RADM2 chemical mechanism is "outdated" in the
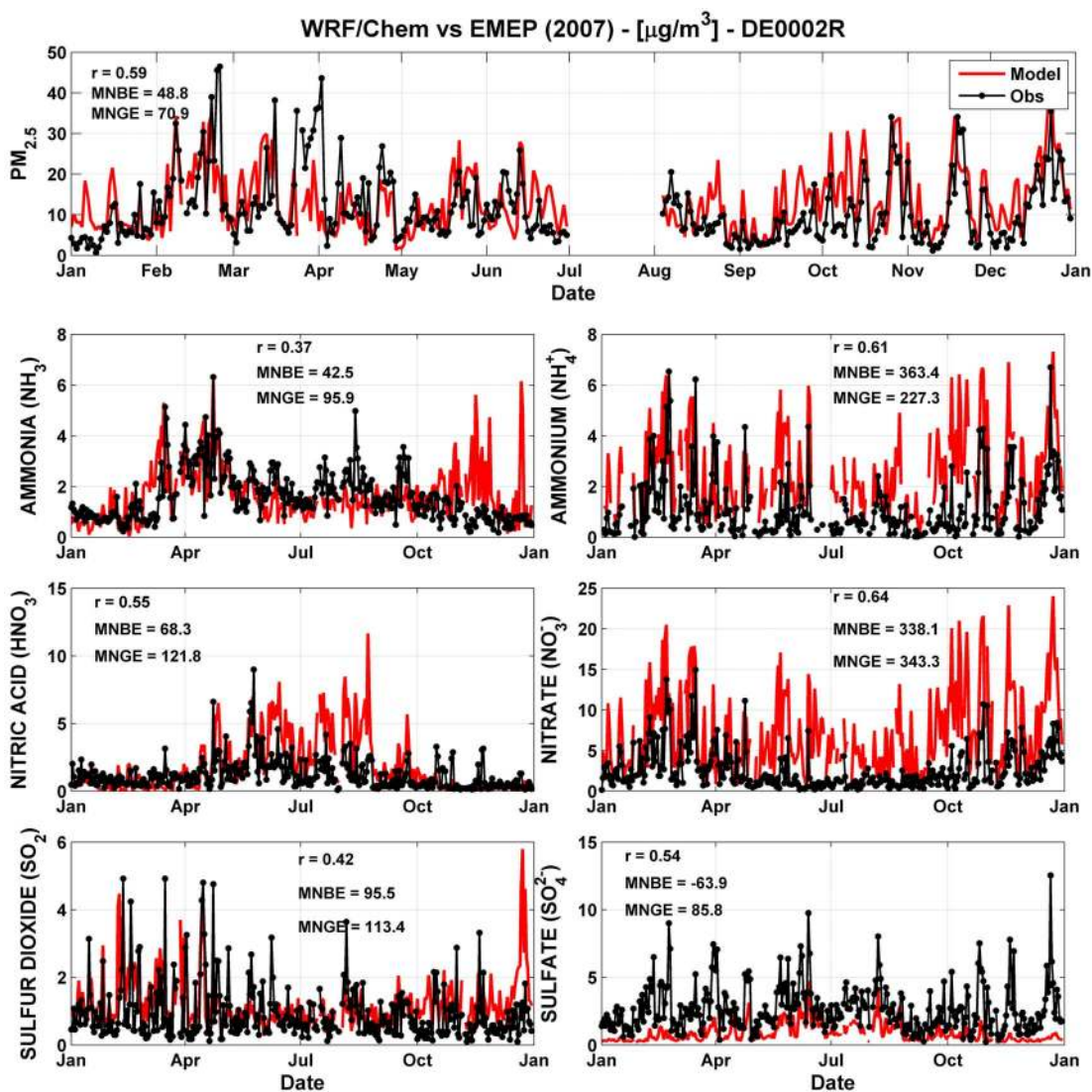
Figure 7. Simulated and observed time series of daily $PM_{2.5}$, ammonia (NH_3), nitric acid (HNO_3), sulfur dioxide (SO_2), ammonium (NH_4^+), nitrate (NO_3^-) and sulphate ($SO_4^=$) at Langenbrügge station (DE0002R, Germany).

treatment of SOA. RADM2 does not include the oxidation of biogenic monoterpenes and has a limited treatment of anthropogenic VOC oxidation [*McKeen et al.*, 2007]. *Bessagnet et al.* [2008] estimated that over Europe the contribution of biogenic SOA to the total mass of SOA is of 75–95%. *Aksoyoglu et al.* [2011] with a modeling study shown that over Switzerland the 30–50% of SOA are formed from monoterpenes. This is a gap that warrants future work for WRF/Chem development. We also remind the reader that other chemical mechanism (e.g., RACM, CBM-Z, SAPRC) with a more complex treatment of VOC oxidation and SOA production with respect to RADM2 are already implemented in WRF/Chem.

[38] Another possible source of negative bias could be linked to unspeciated $PM_{2.5}$ due to underestimation of its emissions. An indicative value of primary $PM_{2.5}$ is calculable from the difference of total gravimetric $PM_{2.5}$ and the sum of total carbon and inorganic mass. However, we do not have enough EC and OC data here to deepen the analysis.

[39] Another potential source of the $PM_{2.5}$ bias is the simulation of the meteorological fields. In a high resolution study, *Aksoyoglu et al.* [2011] quantified how aerosol mass concentration varies locally, when modeled temperature and wind speed are modified. They found that when the model temperature is decreased by 5°C the nitrate mass increases up to 5 $\mu g/m^3$; an increase of temperature of the same magnitude induces a decrease of the nitrate concentration of 2–3 $\mu g/m^3$. The SOA amount is almost insensitive to temperature change (up to 0.2 $\mu g/m^3$). The same authors also shown that when the model overestimates the wind speed in low-wind days, a reduction of the modeled wind speed causes an increase of aerosol mass concentration by a factor of 2–3.

[40] Finally, the reader should also consider that the results of this study are obtained with a simplified wet deposition scheme that takes into account only the scavenging of inorganic aerosols in updrafts. A more sophisticated wet deposition module is available in WRF/Chem, but it cannot be not activated separately from aerosol indirect
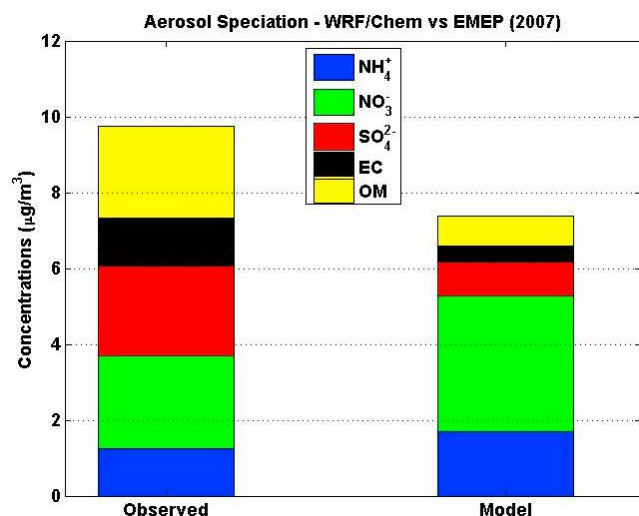
Figure 8. Comparison of observed and modeled domain average aerosol chemical speciation at EMEP monitoring stations. OM is calculated multiplying the observed OC by a factor 1.6.

effects. *Aan de Brugh et al.* [2011] calculated that in the boundary layer the 40% of ammonium and sulphate, 55% of nitrate and 25% of EC and OM is removed by wet scavenging.

3.4. Sensitivity Tests

[41] In this section, we investigate the modeled particulate sulphate underestimation at surface EMEP stations and overprediction of nitrate with some model sensitivity tests. The negative bias of predicted sulphate can be due to several reasons, which we discuss below.

[42] First, the model could underestimate the rate of SO_2 gas phase oxidation. Second, the cloud oxidation of SO_2 is not included in our runs. *McKeen et al.* [2007] found that the models that include aqueous-phase oxidation of sulfur dioxide overestimate sulphate concentrations, and vice versa for those not taking into account this process. *Aan de Brugh et al.* [2011] estimated that 45% of SO_2 aqueous oxidation to sulphate over Europe happens within the boundary layer, thus it may certainly have an important impact on surface concentrations.

[43] Third, another possible explanation is related to boundary layer dynamics. It is known that WRF/Chem can predict an unrealistic nighttime separation of the surface and the upper layers, because the model has a very shallow mixing at night [*McKeen et al.*, 2007]. Since most sources of SO_x are above the nighttime PBL, a weak mixing may deplete surface $SO_4^=$ during night (small production from SO_2).

[44] To explore the three critical points just listed in the two preceding paragraphs, we perform four 1-month sensitivity simulations for February 2007. The choice of this specific month is based on the similarity of particulate inorganic bias with respect to the annual average. Test labels and descriptions are listed in Table 3. The reference run (CTRL) is the simulation we discussed so far. In the first test (KSO2x2), we double the gas-phase oxidation rate of SO_2 by OH to evaluate the impact of this process on sulphate production. For the second test, we note that most of the SO_x EMEP emissions are related to SNAP sectors 1 and 3 (power

Table 3. Description of Sensitivity Simulations in February 2007 to Investigate Inorganic Aerosol Model Bias

Label	Description
CTRL	Reference simulation
KSO2×2	SO_2 gas-phase oxidation rate doubled
SURFEMIS	Power plant and industrial emissions forced at surface level
AQSO2-H2O2	SO_2 aqueous-phase oxidation by H_2O_2 added
AQSO2-O3	SO_2 aqueous-phase oxidation by H_2O_2 and O_3 added

plants and industrial combustion, respectively). About 50% of the flux is localized at 500 m height and the remaining fraction at higher altitude. Therefore, to understand the impact of boundary layer dynamics on surface sulphates, we distribute all the emissions of SNAP 1 and 3 at the surface (SURFEMIS). The last two tests are devoted to aqueous-phase oxidation of SO_2. We add to WRF/Chem the production of SO_4 by SO_2 oxidation in clouds following *Park et al.* [2004]. Within the clouds, the formation of sulphates is limited by the local availability of H_2O_2 and O_3. First we add only the $SO_2+H_2O_2$ reaction (AQSO2-H2O2), then we also consider the oxidation by O_3 (AQSO2-O3).

[45] In Table 4 we report the average inorganic aerosol concentrations calculated at EMEP ground stations in sensitivity tests. The same information is displayed as bar chart in Figure 9.

[46] The first two tests, KSO2x2 and SURFEMIS exhibit an SO_4 enhancement respectively of +28% and +17% with respect to CTRL, but the sulphates are still underestimated with respect to observations. NO_3^- varies by −4% and +4% with respect to CTRL for KSO2x2 and SURFEMIS, respectively, because the small increase of $SO_4^=$ is unable to consume enough ammonia to limit NH_4NO_3 formation in the model. The nitrate increase in SURFEMIS is consistent with the fact that we also bring to the surface additional NO_x emissions related to the SNAP 1 and 3 emission sectors.

[47] The modest increase of sulphate production in first two tests is not surprising, because the lifetime of SO_2 against the oxidation by OH is 7–14 days and SO_2 oxidation occurs mainly in cloud droplets [*Jacob*, 1999]. Indeed, we find a much larger variations of sulphate concentrations in test AQSO2-H2O2 and AQSO2-O3. The simulations indicate that at EMEP stations the SO_2 oxidation in clouds is responsible for 85% of $SO_4^=$ formation. However, comparing AQSO2-O3 results with the observations, we find that

Table 4. Mean Values of Inorganic Aerosol Mass Observed at EMEP Ground-Based Stations in February 2007 and Simulated With WRF/Chem in Sensitivity Test[a]

	NH_4^+ ($\mu g/m^3$)	NO_3^- ($\mu g/m^3$)	$SO_4^=$($\mu g/m^3$)	Total ($\mu g/m^3$)
OBSERVED	1.69 (22.9)	3.56 (48.2)	2.14 (29.0)	7.38
CTRL	2.22 (27.3)	5.34 (65.6)	0.57 (7.0)	8.14
KSO2×2	2.20 (24.4)	5.11 (63.5)	0.73 (9.1)	8.04
SURFEMIS	2.37 (27.5)	5.55 (64.4)	0.67 (8.1)	8.62
AQSO2-H2O2	2.36 (27.9)	4.61 (54.5)	1.49 (17.6)	8.46
AQSO2-O3	2.66 (28.1)	2.94 (31.1)	3.87 (40.9)	9.46

[a]Values in parentheses are percentages of the total. Please refer to Table 3 and text for the description of the tests.
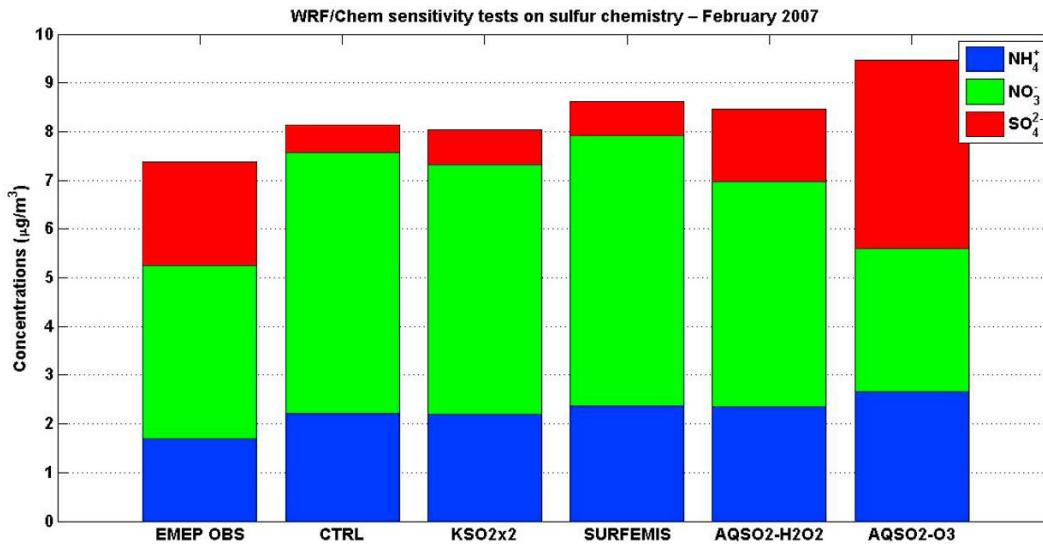
Figure 9. Intercomparison among the average domain of secondary inorganic aerosols simulated in sensitivity tests listed in Table 3 and EMEP observations.

sulphate is overestimated by 81%, ammonium by 57%, and nitrate is underestimated by 17%. Total inorganic aerosol mass is overestimated by 28%.

[48] A useful tool to investigate the skill of the model in converting SO_2 to $SO_4^=$ is the SO_2:total sulphur ratio (S-ratio) [*Stern et al.*, 2008; *Hass et al.*, 2003]. Figure 10 shows the scatter plot of observed and modeled mean S-ratio at EMEP sites, for CTRL, AQSO2-H2O2 and AQSO2-O3. The **r** coefficients are −0.27, 0.38 and 0.49 for CTRL, AQSO2-H2O2 and AQSO2-O3, respectively. The best agreement with measured S-ratio is found for AQSO2-O3, but the S-Ratio tends to be underestimated, i.e. the conversion from SO_2 to

$SO_4^=$ is faster in the model than what really occurs in the atmosphere.

4. Conclusions

[49] The online meteorology-chemistry model WRF/Chem has been implemented over a European domain and evaluated against ground-based and upper air measurements for the year 2007. The aim of the comparison is a first evaluation of model skills over Europe at moderate resolution (30 km) and without the complicating effect of aerosol-cloud-radiation feedbacks in terms of main meteorological and
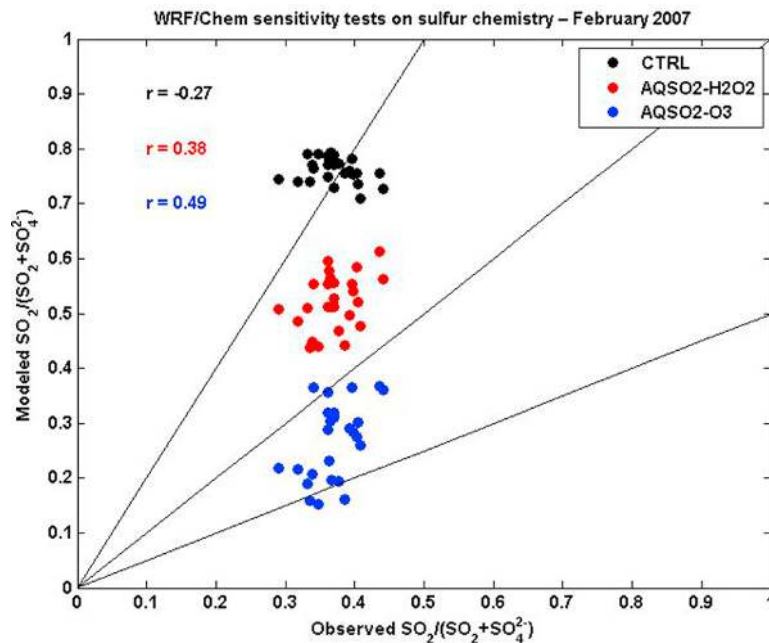
Figure 10. Scatterplot of observed and modeled SO_2:total sulphur ratio (S-ratio) at EMEP site for CTRL, AQSO2-H2O2 and AQSO2-O3 sensitivity tests.

chemical variables. The main step for model implementation over Europe was the development of an interface to the European Monitoring and Evaluation Programme (EMEP) anthropogenic emissions, which we derived from the CHIMERE chemistry-transport model pre-processor [*Bessagnet et al.*, 2008] and adapted to the chemical mechanism of WRF/Chem (see Table 1 and section 2).

[50] WRF/Chem simulates hourly meteorological variables with a mean bias of $-0.1°C$ for temperature and $+8\%$ for relative humidity. Wind speed daily cycle is captured, but the intensity is overestimated by 1.0 m/s. Wind direction has a mean bias of 46°. Comparison with upper-air radiosonde observations displays a bias of the opposite sign with respect to the ground for temperature and humidity, and confirms the overprediction of wind speed throughout the boundary layer.

[51] Hourly ozone daily maxima are underestimated by $-8.6\ \mu g/m^3$ (-4.4%). High negative (positive) bias is found in spring (fall). We argue this might be partially due to an inadequate representation of monthly variability of intercontinental transport through model boundary conditions, which are static climatological profiles in WRF/Chem. Nitrogen dioxide mean values are well reproduced by the model, but highest values of the distribution are not captured.

[52] $PM_{2.5}$ shows a mean bias of -7.3% and a correlation with observations of 0.41 . Model bias is mostly attributable to the higher end of the concentrations distribution. The analysis of the chemical composition of $PM_{2.5}$ and its precursor gases indicates that the model strongly underestimates the carbonaceous fraction, but reproduces the total secondary inorganic fraction. WRF/Chem tends to underestimate the relative amount of secondary organic aerosol (SOA) with respect to total organic mass. This behavior is probably due to the absence of oxidation of monoterpenes and a limited treatment of anthropogenic VOC oxidation in RADM2 mechanism.

[53] Although the total mass is broadly captured by the model, the balance among species in the secondary inorganic fraction differs from observations: sulphate is underestimated by a factor of 2, while nitrate and ammonia are both overestimated by a factor of 2. We carried out several sensitivity tests to better understand this misrepresentation of the particulate inorganic species. Model results suggest that the main player is the missing aqueous-phase oxidation of SO_2 by H_2O_2 and O_3, a process not included in the standard configuration of WRF/Chem without aerosol-clouds feedback. When we add this process, we find a species shift toward more realistic balance, but the conversion from gas to particle of sulphur species, as indicated by the S-ratio, is too fast.

[54] The results obtained in this study show that WRF/Chem performances over Europe are comparable with other state-of-the-art modeling systems, such as those presented in the intercomparisons by *van Loon et al.* [2007] and *Stern et al.* [2008]. In those papers, the models are also set on a continental scale, but with a variety of process parameterizations. Moreover, both EMEP and TNO inventories [*Visscherdijk and Denier van der Gon*, 2005] are used there. This lends confidence in model use as a powerful tool for the study of the aerosol-cloud interactions, but further verification of the aerosol carbonaceous fraction and also the modeled aerosol vertical distribution is recommended. The

introduction of a more complex mechanism for secondary organic aerosol, that includes monoterpene oxidation and an improved treatment of anthropogenic SOA, than what used here (RAMD2/SORGAM), would also be desirable. WRF/Chem community is already moving in this direction, indeed *Shrivastava et al.* [2011] recently implemented in the model a new SOA treatment that takes into account the monoterpene oxidation. Implementation of an option for use of aqueous chemistry and wet deposition schemes without feedbacks is also recommended. Moreover, we point out that WRF/Chem offers several parameterizations for each physical process, several chemical mechanisms and aerosol models. As a consequence, when using a different set-up of the model, the performances may change with respect to those described in this paper. Finally, the future application of WRF/Chem with indirect aerosol effects will be more meaningful at a cloud-resolving scale (say less than 10 km), because the indirect effects are implemented in WRF/Chem only within the microphysics schemes [*Grell et al.*, 2011], thus the implementation of an higher resolution emissions inventory will also be useful.

Appendix A

[55] The statistical indices used to evaluate the model are listed below. Let Obs_i^j and Mod_i^j be the observed and modeled values at time i and station j, respectively. Let N be the number of stations, and $Nobs^j$ the number of observations at station j.

Pearson's Correlation (r) and coefficient of determination (R^2)

$$r = \frac{1}{N}\sum_{j=1}^{N}\frac{1}{Nobs^j - 1}\sum_{i=1}^{Nobs^j} Z_i^j(Mod) \cdot Z_i^j(Obs)$$

$$Z(X) = \frac{X - \langle X \rangle}{\sigma_X}$$

where X is a generic vector and $Z(X)$ is its standard score, also defined above. R^2 is defined as the square of r and denotes the fraction of variability of observations explained by the model.

Mean Bias (MB)

$$MB = \frac{1}{N}\sum_{j=1}^{N}\left(\frac{1}{Nobs^j}\sum_{i=1}^{Nobs^j} Mod_i^j - Obs_i^j\right)$$

Mean Normalized Bias Error (MNBE)

$$MNBE = \frac{1}{N}\sum_{j=1}^{N}\left(\frac{1}{Nobs^j}\sum_{i=1}^{Nobs^j} \frac{Mod_i^j - Obs_i^j}{Obs_i^j}\right) \times 100$$

Mean Normalized Gross Error (MNGE)

$$MNGE = \frac{1}{N}\sum_{j=1}^{N}\left(\frac{1}{Nobs^j}\sum_{i=1}^{Nobs^j} \frac{|Mod_i^j - Obs_i^j|}{Obs_i^j}\right) \times 100.$$

based measurement databases alive and freely accessible. This work was supported by the Italian Space Agency (ASI), in the frame of the QUITSAT (contract I/035/06/0) and PRIMES (contract I/017/11/0) projects, and by the Italian Ministry for University and Research (MIUR), in the frame of the AeroClouds project.

References

Aan de Brugh, J. M. J., M. Schaap, E. Vignati, F. Dentener, F. Kahnert, M. Soviev, V. Huijnen, and M. C. Krol (2011), The European aerosol budget in 2006, *Atmos. Chem. Phys.*, *11*, 1117–1139, doi:10.5194/acp-11-1117-2011.

Ackermann, I. J., H. Hass, M. Memmsheimer, A. Ebel, F. S. Binkowski, and U. Shankar (1998), Modal aerosol dynamics model for Europe: development and first applications, *Atmos. Environ.*, *32*(17), 2981–2999, doi:10.1016/S1352-2310(98)00006-5.

Aksoyoglu, S., J. Keller, I. Barmpadimos, D. Oderbolz, V. A. Lanz, A. S. H. Prévot, and U. Baltensperger (2011), Aerosol modeling in Europe with a focus on Switzerland during summer and winter episodes, *Atmos. Chem. Phys.*, *11*, 7355–7373, doi:10.5194/acp-11-7355-2011.

Andreae, M. O., C. D. Jones, and P. M. Cox (2005), Strong present-day aerosol cooling implies a hot future, *Nature*, *435*, 1187–1190, doi:10.1038/nature03671.

Auvray, M., and I. Bey (2005), Long-range transport to Europe: Seasonal variations and implications for the European ozone budget, *J. Geophys. Res.*, *110*, D11303, doi:10.1029/2004JD005503.

Bessagnet, B., L. Menut, G. Curci, A. Hodzic, B. Guillaume, C. Liousse, S. Moukhtar, B. Pun, C. Seigneur, and M. Schulz (2008), Regional modeling of carbonaceous aerosols over Europe—Focus on secondary organic aerosols, *J. Atmos. Chem.*, *61*, 175–202, doi:10.1007/s10874-009-9129-2.

Carbone, C., et al. (2010), Size-resolved aerosol chimica composition over the Italian Peninsula during typical summer and winter conditions, *Atmos. Environ.*, *44*, 5269–5278, doi:10.1016/j.atmosenv.2010.08.008.

Charlson, R. J., S. E. Schwartz, J. M. Hales, R. D. Cess Jr., J. A. Coakley, J. E. Hansen, and D. J. Hofmann (1992), Climate forcing by anthropogenic aerosols, *Science*, *255*(5043), 423–430, doi:10.1126/science.255.5043.423.

Chen, F., and J. Dudhia (2001), Coupling an advanced land-surface/hydrology model with the Penn State/NCAR MM5 modeling system, Part I: Model description and implementation, *Mon. Weather Rev.*, *129*, 569–585, doi:10.1175/1520-0493(2001)129<0569:CAALSH>2.0.CO;2.

Chin, M., R. B. Rood, S.-J. Lin, J.-F. Müller, and A. M. Thompson (2000), Atmospheric sulfur cycle simulated in the global model GOCART: Model description and global properties, *J. Geophys. Res.*, *105*, 24,671–24,687, doi:10.1029/2000JD900384.

Chou, M.-D., M. J. Suarez, C.-H. Ho, M. M.-H. Yan, and K.-T. Lee (1998), Parameterizations for cloud overlapping and shortwave single-scattering properties for use in general circulation and cloud ensemble models, *J. Clim.*, *11*, 202–214, doi:10.1175/1520-0442(1998)011<0202:PFCOAS>2.0.CO;2.

Curci, G. (2012), On the impact of time-resolved boundary conditions on the simulation of surface ozone and PM$_{10}$, in *Air Pollution Book 2*, edited by M. Khare, InTech Open Access, Rijeka, Croatia, in press.

de Meij, A., M. Krol, F. Dentener, E. Vignati, C. Cuvelier, and P. Thunis (2006), The sensitivity of aerosol in Europe to two different emission inventories and temporal distribution of emissions, *Atmos. Chem. Phys.*, *6*, 4287–4309, doi:10.5194/acp-6-4287-2006.

Fast, J. D., Jr., W. I. Gustafson, R. C. Easter, R. A. Zaveri, J. C. Barnard, E. G. Chapman, G. A. Grell, and S. E. Peckham (2006), Evolution of ozone, particulate, and aerosol direct radiative forcing in the vicinity of Houston using a fully coupled meteorology-chemistry-aerosol model, *J. Geophys. Res.*, *111*, D21305, doi:10.1029/2005JD006721.

Friedrich, R. (1997), GENEMIS: Assessment, improvement, temporal and spatial disaggregation of European emission data, in *Tropospheric Modelling and Emission Estimation, Part 2*, edited by A. Ebel, R. Friedrich, and H. Rhode, pp. 181–214, Springer, New York.

Gelencsér, A., B. May, D. Simpson, A. Sanchez-Ochoa, A. Kasper-Giebl, H. Puxbaum, A. Caseiro, C. Pio, and M. Legrand (2007), Source apportionment of PM$_{2.5}$ organic aerosol over Europe: primary/secondary, natural/anthropogenic, and fossil/biogenic origin, *J. Geophys. Res.*, *112*, D23S04, doi:10.1029/2006JD008094.

Grell, G. A., and D. Devenyi (2002), A generalized approach to parameterizing convection combining ensemble and data assimilation techniques, *Geophys. Res. Lett.*, *29*(14), 1693, doi:10.1029/2002GL015311.

Grell, G. A., R. Knoche, S. E. Peckham, and S. A. McKeen (2004), Online versus offline air quality modeling in cloud-resolving scales, *Geophys. Res. Lett.*, *31*, L16117, doi:10.1029/2004GL020175.

Grell, G. A., S. E. Peckham, S. McKeen, R. Schmitz, G. Frost, W. C. Skamarock, and B. Eder (2005), Fully coupled "online" chemistry within the WRF model, *Atmos. Environ.*, *39*, 6957–6975, doi:10.1016/j.atmosenv.2005.04.027.

Grell, G., S. R. Freitas, M. Stuefer, and J. Fast (2011), Inclusion of biomass burning in WRF-Chem: Impact of wildfires on weather forecasts, *Atmos. Chem. Phys.*, *11*, 5289–5303, doi:10.5194/acp-11-5289-2011.

Guenther, A. B., P. Zimmerman, P. C. Harley, R. K. Monson, and R. Fall (1993), Isoprene and monoterpene emission rate variability: model evaluations and sensitivity analyses, *J. Geophys. Res.*, *98*, 12,609–12,617, doi:10.1029/93JD00527.

Guenther, A. B., P. Zimmerman, and M. Wildermuth (1994), Natural volatile organic compound emission rate estimates for US woodland landscape, *Atmos. Environ.*, *28*, 1197–1210, doi:10.1016/1352-2310(94)90297-6.

Hansen, J., M. Sato, and R. Ruedy (1997), Radiative forcing and climate response, *J. Geophys. Res.*, *102*, 6831–6864, doi:10.1029/96JD03436.

Hass, H., M. Van Loon, C. Kessler, J. Matthijsen, F. Sauter, R. Stern, R. Zlatev, J. Langner, V. Fortescu, and M. Schaap (2003), Aerosol modeling: results and intercomparison from European Regional-scale Modeling Systems: A contribution to the EUROTRAC-2 Subproject GLOREAM, *Spec. Rep. EUROTRAC-2*, ISS, Munich, Germany.

Jacob, D. J. (1999), *Introduction to Atmospheric Chemistry*, 266 pp., Princeton Univ. Press, Princeton, N. J.

Jimenez, J. L., et al. (2009), Evolution of organic aerosols in the atmosphere, *Science*, *326*, 1525–1529, doi:10.1126/science.1180353.

Kasibhatla, P., and W. L. Chameides (2000), Seasonal modeling of regional ozone pollution in the eastern United States, *Geophys. Res. Lett.*, *27*, 1415–1418, doi:10.1029/1999GL011147.

Krol, M., S. Houweling, B. Bregman, M. van den Broek, A. Segers, P. van Velthoven, W. Peters, F. Dentener, and P. Bergamaschi (2005), The two-way nested global chemistry-transport zoom model TM5: algorithm and applications, *Atmos. Chem. Phys.*, *5*(2), 417–432, doi:10.5194/acp-5-417-2005.

Langmann, B., S. Varghese, E. Marmer, E. Vignati, J. Wilson, P. Stier, and C. O'Dowd (2008), Aerosol distribution over Europe: A model evaluation study with detailed aerosol microphysics, *Atmos. Chem. Phys.*, *8*, 1591–1607, doi:10.5194/acp-8-1591-2008.

Legrand, M., and H. Puxbaum (2007), Summary of the CARBOSOL project: Present and retrospective state of organic versus inorganic aerosol over Europe, *J. Geophys. Res.*, *112*, D23S01, doi:10.1029/2006JD008271.

Lin, Y.-L., R. D. Farley, and H. D. Orville (1983), Bulk parameterization of the snow field in a cloud model, *J. Clim. Appl. Meteorol.*, *22*, 1065–1092, doi:10.1175/1520-0450(1983)022<1065:BPOTSF>2.0.CO;2.

Liu, S. C., et al. (1996), Model study of tropospheric trace species distributions during PEM-West A, *J. Geophys. Res.*, *101*, 2073–2085, doi:10.1029/95JD02277.

Lohmann, H., and J. Feichter (2005), Global indirect effects: A review, *Atmos. Chem. Phys.*, *5*, 715–737, doi:10.5194/acp-5-715-2005.

Mathur, R., S. Yu, D. Kang, and K. L. Schere (2008), Assessment of the wintertime performance of developmental particulate matter forecast with the Eta-Community Multiscale Air Quality modeling system, *J. Geophys. Res.*, *113*, D02303, doi:10.1029/2007JD008580.

McKeen, S., et al. (2005), Assessment of an ensemble of seven real-time ozone forecasts over eastern North America during the summer of 2004, *J. Geophys. Res.*, *110*, D21307, doi:10.1029/2005JD005858.

McKeen, S., et al. (2007), Evaluation of several PM$_{2.5}$ forecast models using data collected during the ICARTT/NEAQS 2004 field study, *J. Geophys. Res.*, *112*, D10S20, doi:10.1029/2006JD007608.

Memmesheimer, M., E. Friese, A. Ebel, H. J. Jakobs, H. Feldmann, C. Kessler, and G. Piekorz (2004), Long-term simulations of particulate matter in Europe on different scales using sequential nesting of a regional model, *Int. J. Environ. Pollut.*, *22*, 108–132.

Meng, Z., D. Dabdud, and J. H. Seinfeld (1997), Chemical coupling between atmospheric ozone and particulate matter, *Science*, *277*, 116–119, doi:10.1126/science.277.5322.116.

Middleton, P., W. R. Stockwell, and W. P. Carter (1990), Aggregation and analysis of volatile organic compound emissions for regional modelling, *Atmos. Environ.*, *24*, 1107–1133, doi:10.1016/0960-1686(90)90077-Z.

Mircea, M., M. D'Isidoro, A. Maurizi, L. Vitali, G. Monforti, G. Zanini, and F. Tampieri (2008), A comprehensive performance evaluation of the air quality model BOLCHEM to reproduce the ozone concentrations over Italy, *Atmos. Environ.*, *42*(6), 1169–1185, doi:10.1016/j.atmosenv.2007.10.043.

Misenis, C., and Y. Zhang (2010), An examination of sensitivity of WRF/Chem predictions to physical parameterizations, horizontal grid spacing, and nesting options, *Atmos. Res.*, *97*, 315–334, doi:10.1016/j.atmosres.2010.04.005.

Mlawer, E. J., S. J. Taubaman, P. D. Brown, M. J. Iacono, and S. A. Clough (1997), Radiative transfer for inhomogeneous atmosphere: RRTM, a validated correlated-k model for the longwave, *J. Geophys. Res.*, *102*(D14), 16,663–16,682, doi:10.1029/97JD00237.

Nakanishi, M., and H. Niino (2006), An improved Mellor-Yamada Level-3 Model: Its numerical stability and application to a regional prediction of advection fog, *Boundary Layer Meteorol.*, *119*, 397–407, doi:10.1007/s10546-005-9030-8.

Park, R. J., D. J. Jacob, D. B. Field, R. M. Yantosca, and M. Chin (2004), Natural and transboundary pollution influences on sulphate-nitrate-ammonium aerosol in the United States: Implication for policy, *J. Geophys. Res.*, 109, D15204, doi:10.1029/2003JD004473.

Passant, N. (2002), Speciation of UK emissions of NMVOC, *AEAT/ENV/0545*, AEA Technology, London.

Pio, C. A., et al. (2007), Climatology of aerosol composition (organic versus inorganic) at nonurban sites on a west–east transect across Europe, *J. Geophys. Res.*, 112, D23S02, doi:10.1029/2006JD008038.

Pope, C. A. (2000), Review: Epidemiological basis for particulate air pollution health standards, *Aerosol Sci. Technol.*, 32, 4–14, doi:10.1080/027868200303885.

Putaud, J. P., et al. (2004), A European aerosol phenomenology—2. Chemical characteristics of particulate matter at kerbside, urban, rural and background sites in Europe, *Atmos. Environ.*, 38, 2579–2595, doi:10.1016/j.atmosenv.2004.01.041.

Putaud, J. P., et al. (2010), A European aerosol phenomenology—3: Physical and chemical characteristics of particulate matter from 60 rural, urban, and kerbside sites across Europe, *Atmos. Environ.*, 44, 1308–1320, doi:10.1016/j.atmosenv.2009.12.011.

Rosenfeld, D., U. Lohmann, G. B. Raga, C. D. O'Dowd, M. Kulmala, S. Fuzzi, A. Reissell, and M. O. Andreae (2008), Flood or drought: how do aerosols affect precipitation?, *Science*, 321, 1309, doi:10.1126/science.1160606.

Sartelet, K. N., E. Debry, K. Fahey, Y. Roustan, M. Tombette, and B. Sportisse (2007), Simulation of aerosols and gas-phase species over Europe with the POLYPHEMUS system: Part I—Model-to-data comparison for 2001, *Atmos. Environ.*, 41, 6116–6131, doi:10.1016/j.atmosenv.2007.04.024.

Schaap, M., F. Sauter, R. Timmermans, M. Roemer, G. Velders, J. Beck, and P. Builtjes (2008), The LOTOS-EUROS model: description, validation and latest developments, *Int. J. Environ. Pollut.*, 32(2), 270–290, doi:10.1504/IJEP.2008.017106.

Schell, B., I. J. Ackermann, H. Hass, F. S. Binkowski, and A. Ebel (2001), Modeling the formation of secondary organic aerosol within a comprehensive air quality model system, *J. Geophys. Res.*, 106, 28,275–28,293, doi:10.1029/2001JD000384.

Schmid, H., et al. (2001), Results of the "carbon conference" international aerosol carbon round robin test stage 1, *Atmos. Environ.*, 35, 2111–2121, doi:10.1016/S1352-2310(00)00493-3.

Schürmann, G. J., A. Algieri, I. M. Hedgecock, G. Manna, N. Pirrone, and F. Sprovieri (2009), Modelling local and synoptic scale influences of ozone concentrations in a topographically complex region of Southern Italy, *Atmos. Environ.*, 43, 4424–4434, doi:10.1016/j.atmosenv.2009.06.017.

Seinfeld, J. H., and S. Pandis (2006), *Atmospheric Chemistry and Physics: From Air Pollution to Climate Change*, 2nd ed., 1203 pp., John Wiley, Hoboken, N. J.

Shaw, W. J., K. J. Allwine, B. G. Fritz, F. C. Rutz, J. P. Rishel, and E. G. Chapman (2008), An evaluation of the wind erosion module in DUSTRUN, *Atmos. Environ.*, 42, 1907–1921, doi:10.1016/j.atmosenv.2007.11.022.

Shrivastava, M., J. Fast, R. Easter, W. I. Gustafson Jr., R. A. Zaveri, J. L. Jimenez, P. Saide, and A. Hodzic (2011), Modeling organic aerosols in a megacity: Comparison of simple and complex representations of the volatility basis set approach, *Atmos. Chem. Phys.*, 11, 6639–6662, doi:10.5194/acp-11-6639-2011.

Simpson, D., H. Fagerli, J. E. Jonson, S. Tsyro, P. Wind, and J.-P. Tuovinen (2003), Transboundary acidification, eutrophication and ground level ozone in Europe. Part I: Unified EMEP model description, *EMEP Rep. 1/2003*, 104 pp., Norw. Meteorol. Inst., Oslo.

Stern, R., R. Yamartino, and A. Graff (2006), Analyzing the response of a chemical transport model to emissions reductions utilizing various grid resolutions, paper presented at 28th International Technical Meeting on Air Pollution Modelling and Its Application, NATO, Leipzig, Germany.

Stern, R., et al. (2008), A model inter-comparison study focussing on episode with elevated PM10 concentrations, *Atmos. Environ.*, 42, 4567–4588, doi:10.1016/j.atmosenv.2008.01.068.

Stockwell, W. R., P. Middleton, J. S. Chang, and X. Tang (1990), The second-generation regional acid deposition model chemical mechanism for regional air quality modeling, *J. Geophys. Res.*, 95, 16,343–16,367, doi:10.1029/JD095iD10p16343.

Tie, X., F. Geng, L. Peng, W. Gao, and C. Zhao (2009), Measurement and modeling of O_3 variability in Shanghai, China: Application of the WRF/Chem model, *Atmos. Environ.*, 43, 4289–4302, doi:10.1016/j.atmosenv.2009.06.008.

Turpin, B. J., and H.-J. Lim (2001), Species contributions to $PM_{2.5}$ mass concentrations: Revisiting common assumptions for estimating organic mass, *Aerosol Sci. Technol.*, 35, 602–610.

Van Dingenen, R., et al. (2004), A European aerosol phenomenology—1: Physical characteristic of particulate matter at kerbside, urban, rural and background sites in Europe, *Atmos. Environ.*, 38, 2561–2577, doi:10.1016/j.atmosenv.2004.01.040.

van Loon, M., et al. (2007), Evaluation of long-term ozone simulations from seven regional air quality models and their ensemble, *Atmos. Environ.*, 41, 2083–2097, doi:10.1016/j.atmosenv.2006.10.073.

Vautard, R., et al. (2007), Evaluation and intercomparison of ozone and PM10 simulations by several chemistry transport models over four European cities within the CityDelta project, *Atmos. Environ.*, 41, 173–188, doi:10.1016/j.atmosenv.2006.07.039.

Vestreng, V. (2003), Review and revision: Emission data reported to CLRTAP, *EMEP/MSC-W Note 1/2003*, 134 pp., Norw. Meteorol. Inst., Oslo. [Available at http://emep.int/publ/reports/2003/mscw_note_1_2003.pdf.]

Vignati, E., M. Karl, M. Krol, J. Wilson, P. Stier, and F. Cavalli (2010), Sources of uncertainties in modelling black carbon at the global scale, *Atmos. Chem. Phys.*, 10, 2595–2611, doi:10.5194/acp-10-2595-2010.

Visscherdijk, A. J. H., and H. A. C. Denier van der Gon (2005), Gridded European anthropogenic emission data for NO_x, SO_2, NMVOC, NH_3, CO, PM_{10}, $PM_{2.5}$ and CH_4 for the year 2000, *TNO-Rep. B&O-AR 2005/106*, 90 pp., Neth. Org. for Appl. Sci. Res., Apeldoorn, Netherlands.

Wang, X., et al. (2010), WRF-Chem simulation of East Asian air quality: Sensitivity to temporal and vertical emissions distributions, *Atmos. Environ.*, 44, 660–669, doi:10.1016/j.atmosenv.2009.11.011.

Wesely, M. L. (1989), Parameterization of surface resistance to gaseous dry deposition in regional-scale numerical models, *Atmos. Environ.*, 23, 1293–1304, doi:10.1016/0004-6981(89)90153-4.

Wild, O., X. Zhu, and M. J. Prather (2000), Fast-J: Accurate simulation of in- and below cloud photolysis in tropospheric chemical models, *J. Atmos. Chem.*, 37, 245–282, doi:10.1023/A:1006415919030.

Wilson, R., and J. D. Spengler (1996), *Particles in Our Air: Concentrations and Health Effects*, Harvard Univ. Press, Cambridge, Mass.

Yttri, K. E., et al. (2007), Elemental and organic carbon in PM_{10}: A one year measurement campaign within the European Monitoring and Evaluation Program EMEP, *Atmos. Chem. Phys.*, 7, 5711–5725, doi:10.5194/acp-7-5711-2007.

Yu, S., R. Mathur, K. Schere, D. Kang, J. Pleim, J. Young, D. Tong, G. Pouliot, S. A. McKeen, and S. T. Rao (2008), Evaluation of real-time $PM_{2.5}$ forecasts and process analysis for $PM_{2.5}$ formation over the eastern United States using the Eta-CMAQ forecast model during the 2004 ICARTT study, *J. Geophys. Res.*, 113, D06204, doi:10.1029/2007JD009226.

Zaveri, R. A., and L. K. Peters (1999), A new lumped structure photochemical mechanism for large-scale applications, *J. Geophys. Res.*, 104, 30,387–30,415, doi:10.1029/1999JD900876.

Zaveri, R. A., R. C. Easter, J. D. Fast, and K. L. Peters (2008), Model for Simulating Aerosol Interaction and Chemistry (MOSAIC), *J. Geophys. Res.*, 113, D13204, doi:10.1029/2007JD008782.

Zhang, Y. (2008), Online-coupled meteorology and chemistry models: History, current status, and outlook, *Atmos. Chem. Phys.*, 8, 2895–2932, doi:10.5194/acp-8-2895-2008.

Zhang, Y., and M. K. Dubey (2009), Comparison of WRF/Chem simulated O_3 concentrations in Mexico City with ground-based RAMA measurements during the MILAGRO period, *Atmos. Environ.*, 43, 4622–4631, doi:10.1016/j.atmosenv.2009.05.039.

Zhang, Y., X.-Y. Wen, and C. J. Jang (2010), Simulating chemistry-aerosol-cloud-radiation-climate feedbacks over the continental U.S. using online-coupled Weather Research Forecasting Model with Chemistry (WRF/Chem), *Atmos. Environ.*, 44, 3568–3582, doi:10.1016/j.atmosenv.2010.05.056.

B. Bessagnet, Institut National de l'Environnement Industriel et des Risques, Parc Technologique ALATA, F-60550 Verneuil en Halatte, France.

G. Curci, P. Tuccella, and G. Visconti, CETEMPS, Department of Physics, University of L'Aquila, Via Vetoio, I-67010 Coppito, L'Aquila, Italy. (paolo.tuccella@aquila.infn.it)

L. Menut, Laboratoire de Météorologie Dynamique, Institut Pierre-Simon Laplace, Ecole Polytechnique, F-91128 Palaiseau, France.

R. J. Park, School of Earth and Environmental Sciences, Seoul National University, San 56-1, Sillimdong, Gwanakgu, Seoul 151-742, South Korea.